

Synthesis and Characterization of Hydroxy-Bisphosphonate Micrometer-Sized Particles by Dispersion Polymerization of a New Styrylbisphosphonate Monomer

Ravit Chen, Jenny Goldshtein, Shlomo Margel

Department of Chemistry, Institute of Nanotechnology and Advanced Materials, Bar-Ilan University, Ramat-Gan 52900, Israel
Correspondence to: R. Chen (E-mail: ravitc@iibr.gov.il; ravit.chen244@gmail.com); on sabbatical leave from the Israel Institute for Biological Research, Organic Chemistry Department P.O. Box 19, Ness-Ziona 74100, Israel)

Received 13 December 2012; accepted 25 January 2013; published online 19 February 2013

DOI: 10.1002/pola.26601

ABSTRACT: Bisphosphonates (BPs) are nonhydrolyzable pyrophosphate (P-O-P) analogs possessing two phosphonate groups linked to a single carbon (P-C-P). The hydroxy-bisphosphonates (hydroxyBPs) are obtained when the hydroxy group is also linked to this bridging carbon. Their ability to form bidentate or tridentate chelates with calcium ions results in a high affinity to hydroxyapatite (HAP) in dentin, enamel and bones. In this study, we designed and prepared cross-linked poly(styrylbisphosphonate) (PStBP) micrometer-sized particles by dispersion polymerization of the styrylbisphosphonate (StBP) and ethylene glycol dimethacrylate (EDMA) monomers. The new StBP monomer was synthesized in an efficient one-pot synthesis using tris(trimethylsilyl)phosphite as the phosphorus source followed by methanolysis. The StBP mono-

mer was successfully isolated and characterized as tri-sodium salt. Polymerization of the StBP monomer was carried out in two steps: in situ conversion of the tri-sodium StBP monomer back to its acid form, followed by radical dispersion polymerization in the presence of the crosslinker EDMA monomer. The resulting crosslinked PStBP micrometer-sized particles retained the unique high affinity of the hydroxy-bisphosphonate side groups to calcium ions and exhibited good adhesive properties to HAP. © 2013 Wiley Periodicals, Inc. *J. Polym. Sci., Part A: Polym. Chem.* **2013**, *51*, 2199–2207

KEYWORDS: biomineralization; crosslinked bisphosphonate particles; dispersions; radical polymerization; styrylbisphosphonate monomer

INTRODUCTION Phosphates and phosphonates exhibit strong interaction with dentin, enamel, and bone owing to their ability to create complexes with calcium ions in the hydroxyapatite (HAP). Therefore, there is an increased interest in using phosphorus-based materials, such as phosphate, O-P(O)(OH)₂, or phosphonate, C-P(O)(OH)₂, acids, or esters in various applications,¹ particularly in the biomedical field, due to their proven biocompatibility.^{2,3}

Several articles have recently described the combination of minerals with phosphorus polymers for bone substitution. For instance, Greish and Brown described the formation of biocompatible organic–inorganic composites by reacting tetracalcium phosphate with poly(vinyl phosphonic acid).⁴ Landfester's group described the formation of hybrid particles via mineralization of calcium phosphate on the surface of a copolymer containing poly(vinylphosphonic acid) or poly(vinylbenzylphosphonic acid) with polystyrene (PS).^{5,6} This group recently illustrated that phosphonate functionalized nanoparticles can be used for biomimetic mineralization of HAP and cellular uptake.⁷ In addition, there is an increasing interest in self-etching adhesive systems in the bonding

of resin composite to enamel or dentin primers containing phosphorus function. Mou et al. described, for the first time, the synthesis and use of phosphorus-containing monomers for dental applications.⁸ They reported that the incorporation of a phosphonic function into monomer structures resulted in increased biocompatibility and adhesion to the tooth because of chelation with calcium ions on the tooth's surface. Subsequently, diverse acrylic monomers containing phosphoric or phosphonic acids were prepared and evaluated as self-etching adhesive systems for potential use in dental applications.^{9–13}

As mentioned, most of the published works in this field relate to phosphates or phosphonate groups while research on bisphosphonic monomers or polymers is very rare. Recently, Avci et al. described the design and synthesis of a bisphosphonic moiety based on methacrylamide or bismethacrylamide monomers and its copolymerization with 2-hydroxyethyl methacrylate.¹⁴

Bisphosphonates (BPs) are chemically stable analogs of inorganic pyrophosphates possessing two phosphonate groups linked to a single carbon (P-C-P).¹⁵ The hydroxy-bisphosphonates (hydroxyBPs) are obtained when a hydroxy group is

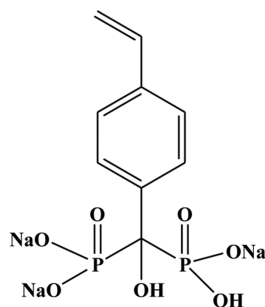


FIGURE 1 Chemical structure of the tri-sodium StBP monomer.

also linked to the bridging carbon. Their ability to form bidentate (BPs) or tridentate (hydroxyBPs) chelates with calcium ions results in a higher affinity to HAP than the mono derivatives.¹⁶ Consequently, BPs and hydroxyBPs form stronger interactions with dentin, enamel, or bone.

In this article, we present the synthesis, characterization, and dispersion polymerization of a new water-soluble styryl-bisphosphonate (StBP) monomer (Fig. 1). This new monomer and its corresponding polymeric particles exhibit three main characteristics: (i) strong interaction with calcium ions due to the hydroxy-bisphosphonate “bone hook,” (ii) rigid structure due to the aromatic ring, and (iii) nonbiodegradability in the body fluids due to the nonhydrolyzable chemical structure of the monomer and the corresponding polymer. The nonbiodegradable StBP monomer and the corresponding particles may be good candidates for various dental and bone applications.

EXPERIMENTAL

Materials

The following analytical grade chemicals were purchased from Sigma-Aldrich, Israel, and used without further purification: 4-vinylbenzoic acid, dry dichloromethane (DCM), dry *N,N*-dimethylformamide (DMF), oxalyl chloride, dry tetrahydrofuran (THF), tris(trimethylsilyl)phosphite, dry methanol, sodium hydroxide, phosphorus pentoxide, ethylene glycol dimethacrylate (EDMA), polyvinylpyrrolidone (PVP, M_w 360,000), potassium persulfate (PPS), concentrated HCl, styrene, sodium dodecyl sulfate (SDS), calcium chloride dihydrate, potassium phosphate, tris buffer (pH 7.4) and HAP “fast flow.” Water was purified by the passage of deionized water through an Elgastat Spectrum reverse osmosis system (Elga, High Wycombe, UK).

Characterization

Infrared spectra were determined on Bruker Platinum-FTIR QuickSnap TM sampling modules A220/D-01. Nuclear magnetic resonance spectroscopy was performed on a Bruker AC 200 MHz spectrometer. ^1H , ^{13}C , and ^{31}P NMR spectra were recorded in deuterium-chloroform or in deuterium oxide solutions. Chemical shifts are reported as parts per million (ppm) downfield from tetramethylsilane, as internal standard in ^1H NMR and ^{13}C NMR and from 85% H_3PO_4 as external standard in ^{31}P NMR. The values are given in δ scale. Solid-state ^{31}P magic angle spin (MAS) NMR spectra were

acquired on a Bruker Avance III 500 MHz spectrometer using a 4-mm VTN CPMAS HX probe at a typical spinning speed of 8 kHz. Elemental analysis was performed, using the Perkin-Elmer 2400 series II Analyzer, by the analytical laboratories of the Hebrew University, Jerusalem. Phosphorus content was determined using the oxygen-flask combustion method and subsequently by ion chromatography analysis using a Dionex IC system. Low-resolution mass spectra were obtained on a Micromass Q-ToF microspectrometer in electrospray mode. High-resolution mass spectrum (HRMS) was obtained on an AutoFlexIII ToF/ToF (Bruker, Germany) in MALDI mode. Hydrodynamic diameter and size distribution of the microparticles dispersed in an aqueous phase were measured using a NANOPHOX particle analyzer (Sympatec, Germany). Surface morphology and dry size diameter were measured with a FEI scanning electron microscope (SEM) (model QUANTA FEG 250). Samples for SEM were prepared by placing a drop of diluted sample on a glass surface and drying it at room temperature. The dried sample was coated with carbon in vacuum before being viewed under SEM. The average size and size distribution of the dry microparticles were determined by measuring the diameter of more than 100 particles with the ANALYSIS Auto (Soft Imaging System, Germany) image analysis software. Transmission electron microscopy (TEM) pictures were obtained with a FEI TECNAI C2 BIOTWIN electron microscope with an accelerating voltage of 120 kV. Samples for TEM were prepared by placing a drop of diluted sample on a 400-mesh carbon-coated copper grid. Thermogravimetric analysis (TGA) was performed with a TGA/DSC 1 STAR^e system (Mettler Toledo, Switzerland). The analysis was performed with ~ 10 mg of dried samples in a nitrogen atmosphere (20 mL min^{-1}) at a heating rate of $10 \text{ }^\circ\text{C min}^{-1}$.

Synthesis and Characterization of the StBP Monomer

The StBP monomer was prepared in three consecutive steps, as described in Figure 2.

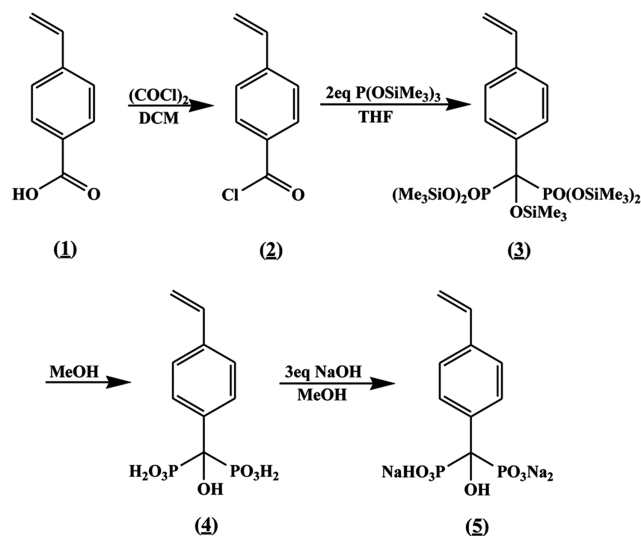


FIGURE 2 Synthesis route of the tri-sodium StBP monomer.

4-Vinylbenzoyl Chloride

4-Vinylbenzoic acid (2.0 g, 13.5 mmol) was dissolved in dry dichloromethane (50 mL) at room temperature under nitrogen atmosphere. DMF (1 drop) was added as a catalyst, followed by oxalyl chloride (3.0 mL). The reaction mixture was stirred at room temperature overnight. The resulting mixture (light yellow) was evaporated to dryness, yielding clear yellow oil.

ATR (neat): 3090–3010 (s, *p*-disubstitute aromatic ring), 1769, 1739 (s, C=O), 1601 (s, CH=CH), 1564, 1404 (s, aromatic ring) 1209 1170 (band, *p*-disubstitute aromatic ring) 991, 922, 874, 848 (band, CH aromatic) 662, 612 cm⁻¹ (s, C–Cl).

Pentakis(trimethylsilyl) Hydroxyl (4-vinylphenyl) Methylenebisphosphonate

4-Vinylbenzoyl chloride (13.5 mmol) was dissolved in dry THF (50 mL) followed by drop wise addition at room temperature of tris(trimethylsilyl) phosphite (10.0 mL, 29.7 mmol). The reaction mixture was stirred overnight at room temperature and was evaporated to dryness, yielding a yellowish solid.

ATR (neat): 3080–2960 (s, *p*-disubstitute aromatic ring CH), 1601 (s, CH=CH), 1492, 1452 (s, aromatic ring) 1254 (s, Si–CH₃) 1230, 1180 (s, P=O), 1052 (s, P–O), 846 (band *p*-disubstitute aromatic ring), 760 (s, C–Si), 697 (P–C), 534 cm⁻¹ (O–P–O). ³¹P NMR (200 MHz, CDCl₃, δ): 7.6 ppm.

Tri-sodium Hydroxyl (4-vinylphenyl) Methylenebisphosphonate (Tri-sodium StBP)

Pentakis(trimethylsilyl) hydroxyl (4-vinylphenyl) methylenebisphosphonate was taken up in 20 mL of absolute methanol, followed immediately by the addition of a filtered solution of sodium hydroxide (1.62 g, 40.5 mmol) in methanol (40 mL). The flask of the sodium hydroxide methanol solution and the filter paper were washed with an additional amount of dry methanol (10 mL). The reaction mixture was stirred for 2 h at room temperature. The product was collected by filtration, washed with methanol, and dried in a desiccator containing phosphorus pentoxide under vacuum (2 mmHg). The dried product was obtained as 4.8 g (88%) white powder.

IR (KBr) (neat): 3629 (v, OH), 3000–3100 (s, *p*-disubstitute aromatic ring CH), 1600–1670 (s, CH=CH, band OH), 1508 (s, aromatic ring) 1402 (s, OH) 1174, 1093 (antisymmetric stretch PO₃⁻) 970, 918 (symmetric stretch PO₃⁻) 827 (band *p*-disubstitute aromatic ring), 632, 552, 462 cm⁻¹ (band PO₃⁻). ¹P NMR (200 MHz, D₂O, δ): 16.3 ppm (tri-sodium salt). ¹H NMR (200 MHz, D₂O, δ): 7.76 (d, 2H⁴, ³J = 8.0 Hz), 7.48 (d, 2H³, ³J = 8.0 Hz), 6.81 (dd, 1H⁶, CH₂=CH, ³J_{cis} = 11.0 Hz, ³J_{trans} = 17.6 Hz), 5.87 (d, 1H⁷, CH₂=CH, ³J = 17.6 Hz), 5.29 (d, 1H⁷, CH₂=CH, ³J = 10.8 Hz). ¹³C NMR (600 MHz, D₂O, δ): 140.1 (1C, C²), 136.6 (1C, C⁶), 134.8 (1C, C⁵), 126.3 (2C, C⁴), 125.1 (2C, C³), 113.3 (1C, C⁷), 77.5 (t, 1C, C¹, ¹J_{CP} = 127.5 Hz). TOF MS ES⁻: 293 (M-3Na, 100%); 315 (M-2Na, 64%). HRMS MALDI: 292.994. ELEM ANAL: C₉H₉Na₃O₇.

P₂.2.5H₂O (405.1) calculated: C, 26.68; H, 3.48; P, 15.29; experimental C, 26.30; H, 3.33; P, 15.30.

Synthesis of Crosslinked PStBP Microparticles

Crosslinked poly(styrylbisphosphonate) (PStBP) microparticles were formed by dispersion polymerization of the StBP monomer with the crosslinker EDMA monomer. Briefly, particles of 475 ± 71 nm were formed by the dissolution of 294.0 mg StBP monomer, 6.0 mg of EDMA (total monomer 3% w/v), 100 mg PVP (1% w/v) and 30 mg PPS (10% w/v of the monomer) in 9.625 mL deaerated water, followed by the addition of 375 μL of concentrated HCl. The 20-mL vial containing this solution was then shaken at 73 °C for 15 min. The polymerization process was halted by transferring the vial to an ice bath. The formed crosslinked PStBP microparticles were then cleaned of impurities by extensive dialysis (cut off 1,000,000) against water. The polymerization yield of the crosslinked PStBP particles was calculated according to the following equation: weight of the particles/initial weight of the monomers × 100.

Synthesis of PS Microparticles

PS microparticles were formed by emulsion polymerization of the styrene monomer. Briefly, particles of 475 ± 59 nm were formed by adding styrene (2.5 mL) to a deaerated solution of PPS (20 mg) and SDS (72 mg) in water (50 mL). The mixture was then shaken at 73 °C for 18 h. The resulting particles were washed by extensive centrifugation cycles with water and ethanol.

Adsorption of BP on Hydroxyapatite

HAP “fast flow” was equilibrated by suspending 500 mg in 50 mL of 0.05 M Tris buffer (pH 7.4). The suspension was shaken for 24 h at 37 °C. The analyzed product was then added, and the suspensions were shaken for an additional 24 h at 37 °C. The resulting HAP was filtered and dried at ambient temperature in vacuum over phosphor pentoxide. The bisphosphonate adsorbed on the HAP was then analyzed by solid-state ³¹P MAS NMR. The analyzed products were (i) sodium chloride (20 mg, 0.33 mmol) as a negative control, (ii) Alendronate, a commercial BPs compound (109 mg, 0.33 mmol) as a positive control, and (iii) StBP monomer (135 mg, 0.33 mmol).

Hydroxyapatite Mineralization on the Surface of the Crosslinked PStBP Microparticles

Calcium chloride (CaCl₂.2H₂O, 7.74 mM) and potassium phosphate (K₂HPO₄, 4.64 mM) were dissolved separately in 0.05 M tris buffer, pH 7.4. Aqueous suspensions (400 μL, 12 mg mL⁻¹) of the crosslinked PStBP particles (475 ± 71 nm) or PS particles (475 ± 59 nm) were mixed with the potassium phosphate solution (5 mL) in borosilicate glass vials (acid and acetone washed), followed by the addition of the calcium solution (5 mL). The concentration of calcium and phosphate in the formed solution was 9 mM², calcium 3.87 mM, and phosphate 2.32 mM, yielding a mol ratio of [Ca]/[PO₄] of 1.67, as in HAP. The vials were then placed in a shaker (100 rpm) at 37 °C for 24 h. The formed precipitate was filtered, sonicated in fresh water, and then characterized by TEM.

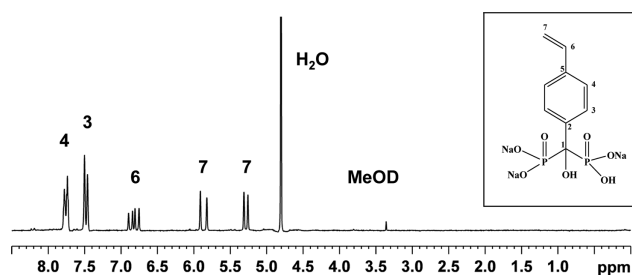


FIGURE 3 ^1H NMR spectrum of the tri-sodium StBP monomer.

RESULTS AND DISCUSSION

Synthesis and Characterization of the StBP Monomer

Several methods have been reported for the synthesis of the 1-hydroxymethylene-1,1-bisphosphonic acids. A common method involves the reaction of a carboxylic acid with phosphorous acid and phosphorus trichloride.^{17–20} In this case, the synthesis is carried out in harsh acidic conditions; consequently it is not suitable for functional substrates like 4-vinylbenzoic acid. The second pathway deals with a multi-step synthesis consisting of three steps:^{21–23} (i) synthesis of the α -ketophosphonate derivatives of the desired compound, (ii) reaction with dialkylphosphite to attain the tetraester intermediate, (iii) hydrolysis of the ester groups to obtain the desired bisphosphonate product. In the present work, we used a mild efficient one-pot synthesis using tris(trimethylsilyl)phosphite as the phosphorus source, previously described by Lecouvey et al.²⁴ This procedure, however, was not yet applied for activated vinylic monomers containing carboxylate groups. Indeed, the bisphosphonate substitution was successfully performed. However, the isolation of the StBP monomer in its acid form was not possible since evaporation of methanol after the methanolysis leads to the formation of a sticky gel, probably due to partial polymerization as already mentioned by Winston et al. regarding the hydroxamic acid monomer.²⁵ We therefore avoided the evaporation of the methanol and produced the StBP monomer by precipitating its tri-sodium salt (Fig. 2). The tri-sodium StBP was isolated by filtration in 88% yield as a white solid, which is soluble only in water. The structure of the tri-sodium StBP monomer was proven by ^1H , ^{13}C , and ^{31}P NMR and FTIR spectroscopies, mass spectrometry and elemental analysis, as shown in the Experimental section. For example, in the ^1H NMR spectrum (Fig. 3) the observed peaks appear in a narrow range (from 7.76 to 5.29 ppm) corresponding to the aromatic and double bond protons. In the ^{13}C NMR spectrum (Fig. 4), the signal of the carbon linked to both a hydroxy and two phosphorus groups appears as a triplet at 77.5 ppm with a coupling constant of 127.5 Hz corresponding to a carbon adjacent to two phosphorus groups. In the ^{31}P NMR spectrum, a singlet appears at 16.6 ppm which is characteristic for hydroxy-bisphosphonate groups [Fig. 5(A)].

Synthesis of the Crosslinked PStBP Microparticles

At first, we attempted to polymerize the tri-sodium StBP monomer by dispersion polymerization in an aqueous continuous phase. The reaction mixture contained the StBP and

EDMA monomers (total amount 3% (w/v)), the PVP stabilizer (1%), and the PPS initiator (10%), all dissolved in deaerated water. The temperature of the reaction mixture was then raised to 73 °C for 18 h. ^1H NMR spectroscopy of the obtained reaction mixture indicated the presence of three unique signals of the protons bound to vinylic carbons at 6.81, 5.87, and 5.29 ppm. The phosphorus signal widths at half maximum remained very sharp, indicating that the mobility of the phosphorus atoms in the solution is high since the solution contains only small molecules. These results indicated that the polymerization of the tri-sodium StBP monomer under these conditions did not occur even after 18 h at 73 °C. We assume that the hydroxy-bisphosphonate function pendant on the styrene moiety is responsible for the polymerization inactivity. The hydroxy-bisphosphonate function might either have affected the reactivity of the double bond or hindered the polymerization process due to steric or negative repulsion forces.

In the published literature, we found a few reports related to the reactivity of phosphonated vinylic monomers. Overberger and Sarlo investigated the reactivity ratios of the phosphonate-containing acrylates in vinyl copolymerization to gain some insight into the influence of the phosphonate group in a radical addition polymerization process.²⁶ They showed that increase of the steric and electron-withdrawing effects of the phosphorous atom leads to lower reactivity of the double bond as compared to methyl acrylate and methyl methacrylate. On the other hand, increasing the distance between the phosphonated group and the double bond leads to better reactivity of the double bond and decreases the steric effect. This can be achieved by introducing the phosphorus group in the *para* position of styrene type monomers, as reported by Boutevin²⁷ and Garner.²⁸ Thus, the aromatic ring served as a bulky and electron rich spacer between the double bond and the phosphorus groups.

Based on these reports, we concluded that the hydroxy-bisphosphonic function is too distal to affect the reactivity of the double bond due to electronic or steric effects. We therefore believe that strong negative repulsion forces exhibited by the tri-sodium bisphosphonate function interfere with the polymerization process. However, this obstacle to polymerizing the tri-sodium StBP monomer with EDMA was easily overcome by *in situ* conversion of the tri-sodium StBP monomer back to its acid form. For this purpose, we prepared a

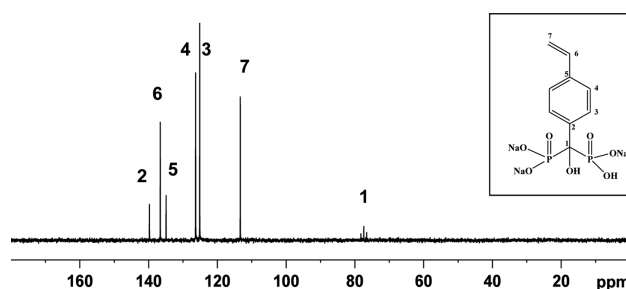


FIGURE 4 ^{13}C NMR spectrum of the tri-sodium StBP monomer.

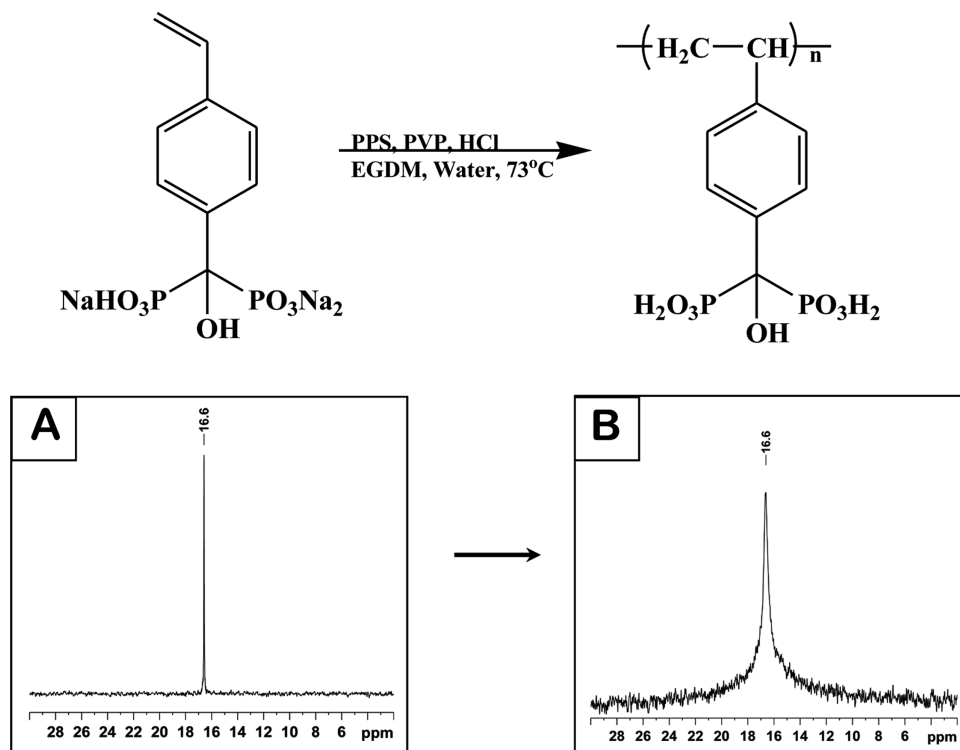


FIGURE 5 Preparation scheme of the crosslinked PStBP particles. ^{31}P NMR spectra of: tri-sodium StBP monomer (A) and polyStBP particles (B) dispersed in deuterium oxide.

reaction mixture containing the tri-sodium StBP and EDMA monomers (total amount 3% (w/v)), the PVP stabilizer (1%), the PPS initiator (10%), and sufficient concentrated hydrochloric acid to convert the sodium salt to the acid form, all dissolved in deaerated water. For the polymerization, the temperature of the reaction mixture was raised to 73 °C for 15 min (Fig. 5). ^{31}P NMR analysis of the suspended crosslinked PStBP micrometer-sized particles in deuterium oxide showed broad signal at 16.6 ppm, indicating the presence of the hydroxy-bisphosphonate functional groups and the low mobility of the phosphorus atoms of the formed particles.

Figure 6 demonstrates the polymerization kinetics of StBP and EDMA prepared according to the description in the above experimental section by measuring the hydrodynamic diameter of the produced particles. Figure 6 shows a marked increase in the size and size distribution of the crosslinked PStBP particles in the first 17 min, followed by the aggregation process after 20 min. For example, for 2, 5, 10, 15, and 17 min following the initiation of the polymerization, the hydrodynamic size and size distribution increased from 230 ± 27 nm to 382 ± 56 , 442 ± 67 , 490 ± 74 , and 550 ± 81 nm, respectively. It should be noted that the highest polymerization yield before the aggregation of the particles occurred was 45%. These experimental results demonstrate a drastic difference in the polymerization ability of the StBP monomer in its acid form compared to its tri-sodium salt form (no polymerization after 18 h). This significant difference supports our theory that strong negative repulsion

forces exhibited by the tri-sodium hydroxy-bisphosphonate function indeed interfere with the polymerization process.

Characterization of the Crosslinked PStBP Microparticles

Figure 7(A) illustrates by a SEM photomicrograph the spherical shape and smooth surface morphology of the crosslinked PStBP particles prepared as described above. The measured hydrodynamic and dry diameter and size distribution of

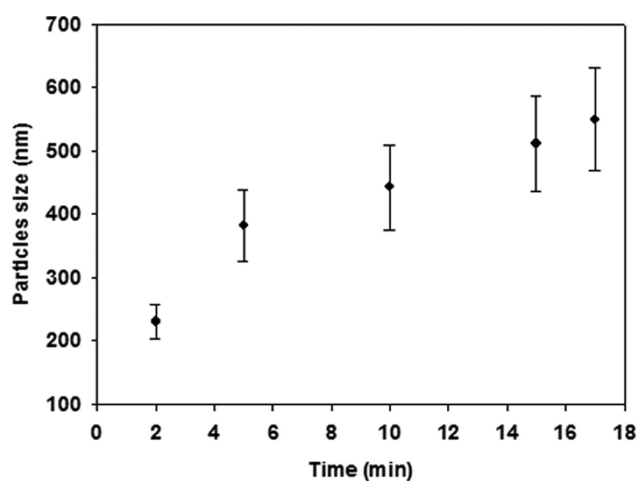


FIGURE 6 Kinetics of the crosslinked PStBP particles formation by following their diameter and size distribution. The crosslinked PStBP particles were prepared in the presence of 3% (w/w) of StBP and EDMA, according to the Experimental section.

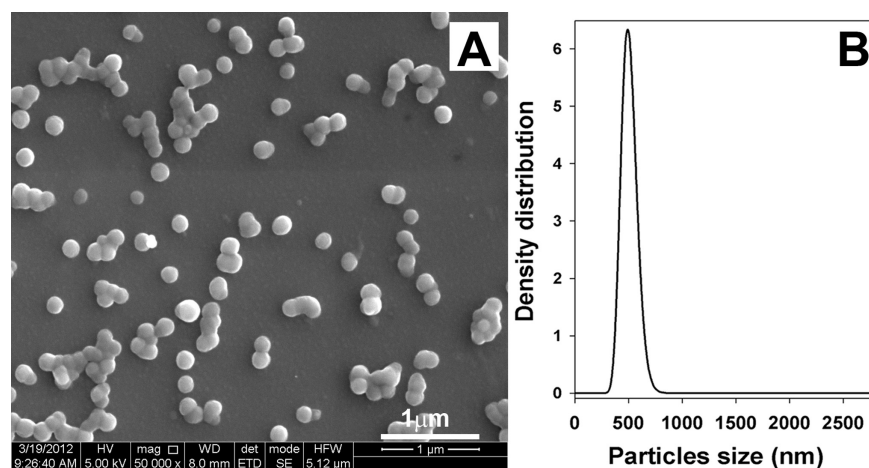


FIGURE 7 SEM image (A) and size histogram (B) of the crosslinked PStBP particles.

these particles are 475 ± 71 and 178 ± 18 nm, respectively (Fig. 7). The hydrodynamic diameters measured by dynamic light scattering (DLS) are larger than those determined by SEM. This is because the DLS technique determines the diameter of solvent-swollen particles whereas the SEM photomicrograph measures the size of particles in the dry state. In water medium, the bisphosphonic acids are in equilibrium with their dissociated form. The polymer chains extend themselves and widen because of the electrostatic repulsion of negative charges. The presence of crosslinking allows for the swelling of the three-dimensional network with polymer dissolution. The hydrophilic nature of the particles probably creates hydrogen bonds with water molecules that significantly enlarge the diameter.^{29,30}

The FTIR spectrum of the monomer demonstrates absorption peaks at 3629 and 1402 cm^{-1} corresponding to vibration and stretching bands of the hydroxyl group, respectively; a broad absorption peak at 1690 – 1600 cm^{-1} corresponding to the double bond stretching band and the OH bending modes;³¹ 1507 cm^{-1} corresponding to the aromatic ring stretching band; 1252 cm^{-1} corresponding to the phosphorus-oxygen double bond stretching band (P=O); 1174 and 1093 cm^{-1} corresponding to antisymmetric stretching bands of the phosphorus group (PO_3^-); 970 and 918 cm^{-1} corresponding to symmetric stretching bands of the phosphorus group (PO_3^-); 827 cm^{-1} corresponding to the vibration bend of the para-di-substitute aromatic ring; 742 cm^{-1} corresponding to the carbon-phosphorus stretching band and 632 , 552 , and 462 cm^{-1} corresponding to the phosphorus group bends (PO_3^-).³² The FTIR spectrum of the crosslinked PStBP particles demonstrates broad absorption peaks similar to those of the monomer, especially for the hydroxy groups at 3200 – 3600 , 1600 – 1690 , and 1400 – 1480 cm^{-1} , and for the phosphonate groups at 1250 , 1179 , 1010 , and 573 cm^{-1} . The significant large absorption of the OH groups of the particles compared to the monomer is also because the FTIR of the monomer was measured for the trisodium StBP, and the FTIR of the crosslinked PStBP particles were measured for the acid form. The new absorption peak

at 2947 cm^{-1} corresponding to CH_2 stretching bands belongs to the hydrocarbon chain created during the polymerization.

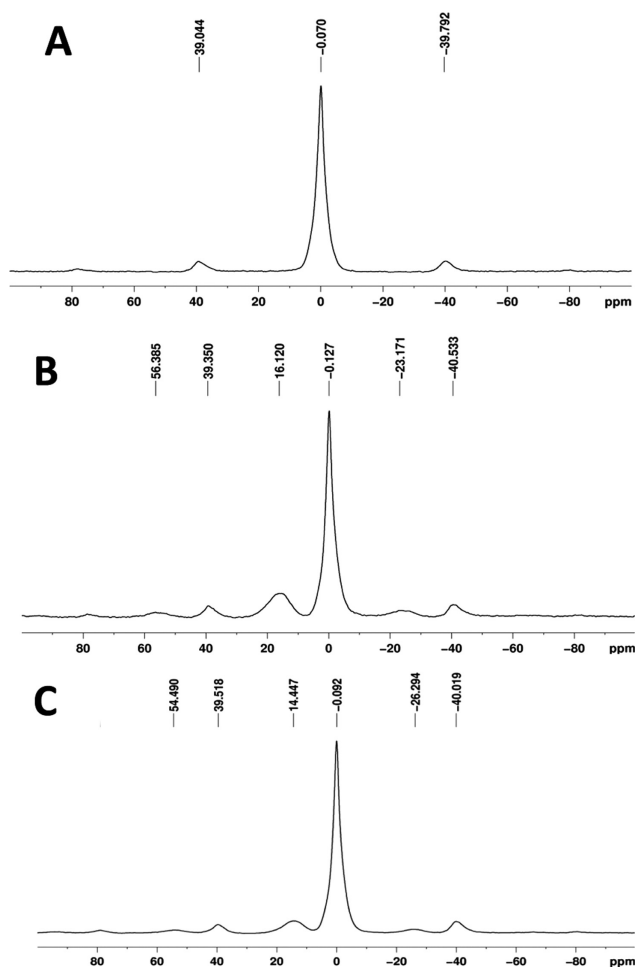


FIGURE 8 Hydroxyapatite adsorbed with (A) sodium chloride, (B) Alendronate, and (C) tri-sodium StBP monomer.

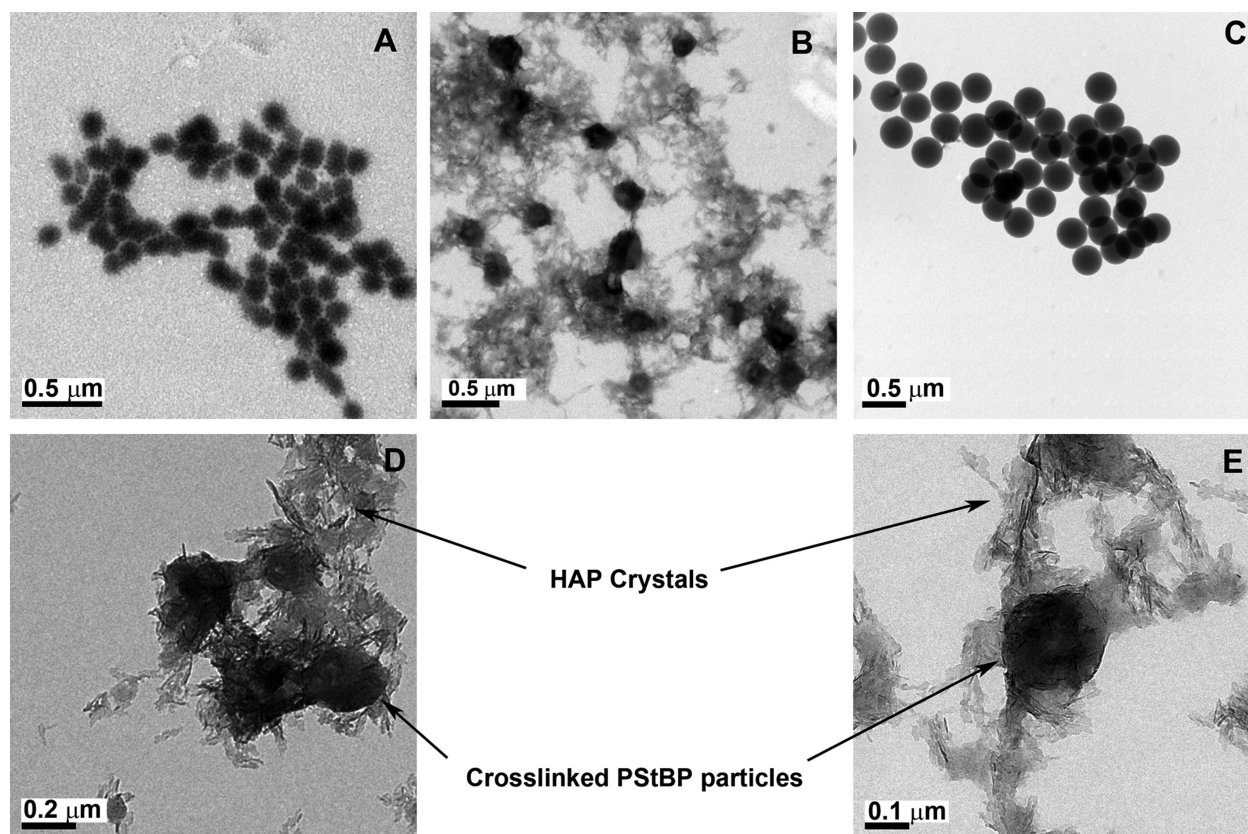


FIGURE 9 TEM photomicrograph images of the crosslinked PStBP particles (A), crosslinked PStBP–HAP hybrid particles (B, D, and E) and PS particles after incubation in supersaturated calcium phosphate solution (C).

Thermogravimetric analyses have been performed to study the thermal stability of the particles. The TGA thermogram of the crosslinked PStBP particles indicates 75% weight loss in three steps. The first step occurs between 95 and 130 °C, indicating a 5% weight loss of the polymer due to evaporation of water traces. This weight loss is demonstrated by a small broad DTG peak at about 100 °C and an endothermic peak at about 100 °C by the DSC curve. The second step occurs at a temperature range between 280 and 360 °C, indicating a 25% weight loss of the polymer. This slope indicates a weight loss resulting from the decomposition of part of the polymer, as confirmed by a strong sharp DTG peak at about 310 °C and a sharp exothermic peak at about 330 °C by the DSC curve. The third step occurs between 360 and 600 °C, illustrating a moderate slope that indicates a 45% weight loss. This behavior is also confirmed by a broad DTG peak range from 360 to 560 °C, which suggests a very slow decomposition process and a broad exothermic peak at the DSC curve. We assume that the decomposition in the second step is due to the decomposition of the aromatic ring of the polymer, similar to the decomposition of PS at that range of temperatures.³³ The slow decomposition process between 360 and 600 °C probably corresponds to the hydroxy-bisphosphonic side groups of the polymer. This step of the polymer decomposition process is exothermic, as indicated by the DSC curve.

Solid-State ³¹P MAS NMR Investigation of the StBP Monomer Adsorbed on HAP

The adsorbed effect and the interaction with HAP of the trisodium StBP monomer were examined based on the method of Grossmann et al.³⁴ Owing to the chemical shift difference between the signals of the HAP and the bisphosphonates, solid-state magic angle spinning (MAS) ³¹P NMR spectroscopy can be used as a preliminary test to observe bisphosphonates adsorbed on HAP. Figure 8(A–C) demonstrates the adsorption effect of hydroxyBPs on HAP. Figure 8(A) shows the adsorption of sodium chloride, serving as negative control, on HAP. Figure 8(B) demonstrates the adsorption of Alendronate, a commercial hydroxyBP, serving as positive control, on HAP. Figure 8(C) shows the adsorption of the trisodium StBP monomer on HAP. The isotropic line at 0 ppm and the sideband at 39 and –40 ppm in Figure 8(A–C) result from HAP. In Figure 8(B,C), in addition to the isotropic line and the sideband of HAP, a broad isotropic line with peaks at 16.1 and 14.4 ppm is observed arising from the Alendronate and StBP monomer signals, respectively. The sideband of the hydroxyBPs derivatives appears in an interval of 40 ppm (56 and –23 ppm for Alendronate and –26 and 54 ppm for the StBP monomer) according to the measured technique. The results indicate that the StBP monomer is adsorbed on HAP similarly to the commercial hydroxyBPs, Alendronate.

Hydroxyapatite Mineralization on the Surface of the Crosslinked PStBP Particles

The study of the adsorbed effect of HAP crystals on the crosslinked PStBP particles was based on Francis³⁵ and Golomb's³⁶ previous works. The principle of this method relies on the ability of the crosslinked PStBP particles to create chelate with the free calcium ions in the supersaturated solution followed by phosphate ions adhesion to the formed HAP-conjugated crosslinked PStBP particles. PS particles, without the hydroxyl-bisphosphonic function, served as a control study for HAP precipitation. Each type of particle, crosslinked PStBP or PS, was shaken at 37 °C in a supersaturated calcium phosphate solution for 24 h. The resulted precipitation was separated and sonicated in fresh water. Samples from this mixture were analyzed by TEM.

Figure 9 illustrates TEM pictures of crosslinked PStBP particles (A), crosslinked PStBP particles after HAP mineralization (B, D, and E) (image E represents a higher magnification of image B) and PS particles after incubation in supersaturated calcium phosphate solution (C). Incubation of the suspended crosslinked PStBP particles resulted in precipitation of crosslinked PStBP-HAP hybrid particles. The first step in the mineralization process is the chelation of the calcium ions by the hydroxy-bisphosphonate's surface groups of the particles. The newly formed calcium-conjugated crosslinked PStBP particles precipitate and grow to be the nuclei of a composed material consisting of the crosslinked PStBP-HAP hybrid particles. In Figure 9(B,D,E), the organic crosslinked PStBP particles are presented as dark, round spots while the inorganic HAP crystals are in white. Figure 9(A) shows that the crosslinked PStBP particles touch each other, probably due to strong hydrogen bonds between the oxygen and the hydrogen atoms of the hydroxyl-bisphosphonic function. Figure 9(B,D,E) illustrates that the crosslinked PStBP particles are surrounded by HAP crystals. As mentioned, this is due to the strong interaction of the crosslinked PStBP particles with the calcium ions. It is interesting to note that in this case the distance between the crosslinked PStBP particles increased relative to the distance shown in Figure 9(A). The increased distance probably results from the ionic bonds formed between the HAP and the hydroxyBPs surface groups of the crosslinked PStBP particles that replace the hydrogen bonds existing between the crosslinked PStBP particles in the absence of HAP. In contrast, most of the PS particles remained suspended in the experimental solution and did not precipitate like the crosslinked PStBP particles. Figure 9(C) exhibits PS particles that did precipitate and which are not surrounded by HAP crystals.

CONCLUSIONS

StBP, a new water-soluble bisphosphonate vinylic monomer, has been synthesized for the first time via an efficient one-pot synthesis. Specifically, 4-vinylbenzyl chloride was reacted with tris(trimethylsilyl)phosphite, followed by methanolysis. Due to the instability of the acid form, the monomer was isolated as a tri-sodium salt. Reproducible dispersion polymerization of StBP with EDMA was achieved after converting, *in*

situ, the tri-sodium salt back to the free acid. The characterization of these crosslinked PStBP particles was accomplished by routine methods such as FTIR, TGA, and DSC. The adsorption effect of the StBP monomer on HAP was examined by solid-state MAS ³¹P NMR spectroscopy and was found to be similar to commercial BPs (Alendronate). The mineralization process of the crosslinked PStBP particles versus PS particles was studied. Only the new hydroxyBPs particles formed crosslinked PStBP-HAP hybrid particles as was demonstrated by TEM images. These results indicate that the StBP monomer and crosslinked PStBP particles have a unique high affinity to HAP. Consequently, these nonbiodegradable StBP monomer and crosslinked PStBP particles may be good candidates for dental and bone applications. For future studies, we plan to extend this work and investigate the efficiency of the StBP monomer and crosslinked PStBP particles for various biomedical applications.

ACKNOWLEDGMENTS

The authors thank Prof. Eli Breuer for fruitful discussions, Dr. Rachel Persky for MS analysis, and Dr. Hugo Gottlieb and Dr. Keren Keinan-Adamsky for NMR analysis.

REFERENCES AND NOTES

- 1 L. Macarie, G. Illia, *Prog. Polym. Sci.* **2010**, *35*, 1078–1092.
- 2 S. Monge, B. Canniccion, A. Graillet, J. J. Robin, *Biomacromolecules* **2011**, *12*, 1973–1982.
- 3 B. Clément, B. Grignard, L. Koole, C. Jérôme, P. Lecomte, *Macromolecules* **2012**, *45*, 4476–4486.
- 4 Y. E. Greish, P. W. Brown, *Biomaterials* **2001**, *22*, 807–816.
- 5 K. Schöller, A. Ethirajan, A. Zeller, K. Landfester, *Macromol. Chem. Phys.* **2011**, *212*, 1165–1175.
- 6 A. Zeller, A. Musyanovych, M. Kappl, A. Ethirajan, M. Dass, D. Markova, M. Klapper, K. Landfester, *Appl. Mater. Interfaces* **2010**, *2*, 2421–2428.
- 7 R. Sauer, P. Froimowicz, K. Schöller, J. M. Cramer, S. Ritz, V. Mailänder, K. Landfester, *Chem. Eur. J.* **2012**, *18*, 5201–5212.
- 8 L. Mou, G. Singh, J. W. Nicholson, *Chem. Commun.* **2000**, 345–346.
- 9 M. A. Bayle, G. Grégoire, P. Sharrock, *J. Dent.* **2007**, *35*, 302–308.
- 10 S. Salman, A. Z. Albayrak, D. Avic, V. Aviyente, *J. Polym. Sci. Part A: Polym. Chem.* **2005**, *43*, 2574–2583.
- 11 D. Avic, L. J. Mathias, *J. Polym. Sci. Part A: Polym. Chem.* **2002**, *40*, 3221–3231.
- 12 G. Sahin, A. Z. Albayrak, Z. Sarayli, D. Avci, *J. Polym. Sci. Part A: Polym. Chem.* **2006**, *44*, 6775–6781.
- 13 N. Moszner, J. Pavlinec, I. Lamparth, F. Zeuner, J. Angermann, *Macromol. Rapid Commun.* **2006**, *27*, 1115–1120.
- 14 B. Akgun, D. Avci, *J. Polym. Sci. Part A: Polym. Chem.* **2012**, *50*, 4854–4863.
- 15 R. G. G. Russell, *Bone* **2011**, *49*, 2–19.
- 16 A. Ebrahimpour, M. D. Francis, In *Bisphosphonate on Bone*; O. L. M. Bijvoet, H. A. Fleisch, R. E. Canfield, R. G. Russell, G., Eds.; Elsevier Science B. V.: Amsterdam, The Netherlands, **1995**; Chapter 8, pp 125–137.
- 17 H. Blum, K. Worms, U.S. Patent 4,054,598, Oct 18, **1977**.

- 18** H. Blum, H. Hempel, K. H. Worms, U.S. Patent 4,267,108, May 12, **1981**.
- 19** E. Bosies, R. Gall, U.S. Patent 4,687,767, Aug 18, **1987**.
- 20** S. Rosini, G. Staibano, U.S. Patent 4,621,077, Nov 4, **1986**.
- 21** D. A. Nicholson, H. Vaughn, *J. Org. Chem.* **1971**, *36*, 3843–3845.
- 22** L. M. Nguyen, E. Niesor, C. L. Bentzen, *J. Med. Chem.* **1987**, *30*, 1426–1433.
- 23** C. L. Bentzen, L. N. Mong, E. Niesor, U.S. Patent 4,416,877 Nov 22, **1983**.
- 24** M. Lecouvey, I. Mallard, T. Bailly, R. Burgada, Y. Leroux, *Tetrahedron Lett.* **2001**, *42*, 8475–8478.
- 25** A. Winston, D. Kirchner, *Macromolecules* **1978**, *11*, 597–603.
- 26** C. G. Overberger, E. Sarlo, *J. Polym. Sci. Part A: Polym. Chem.* **1964**, *2*, 1017–1021.
- 27** B. Boutevin, B. Hamoui, J. P. Parisi, B. Ameduri, *Eur. Polym. J.* **1996**, *32*, 159–163.
- 28** A. Y. Garner, E. C. Chapin, J. G. Abramo, U.S. Patent 3,075,011, **1963**.
- 29** D. Horák, M. Kryštůfek, J. Spěvacek, *J. Polym. Sci. Part A: Polym. Chem.* **2000**, *38*, 653–663.
- 30** P. Riccardo, *J. Macromol. Sci. Chem. Phys.* **1994**, *C34*, 607–662.
- 31** B. Akgun, E. Savci, D. Avci, *J. Polym. Sci. Part A: Polym. Chem.* **2012**, *50*, 801–810.
- 32** M. Mathew, B. O. Fowler, E. Breuer, G. Golomb, I. S. Alferiev, N. Eidelman, *Inorg. Chem.* **1998**, *37*, 6485–6494.
- 33** M. Omer Mizrahi,; S. Margel, *Polymer* **2010**, *51*, 1222–1230.
- 34** G. Grossmann, A. Grossmann, G. Ohms, E. Breure, R. Chen, G. Golomb, H. Cohen, G. Hägele, R. Classen, *Magn. Reson. Chem.* **2000**, *38*, 11–16.
- 35** M. D. Francis, *Calc. Tiss. Res.* **1969**, *3*, 151–162.
- 36** G. Golomb, D. Wagner, *Biomaterials* **1991**, *12*, 397–405.